CLNS 95/1351
CLEO 95-13
August 10, 1995

MEASUREMENTS OF THE RATIOS $\mathcal{B}(D_s^+ \to \eta\ell^+\nu)/\mathcal{B}(D_s^+ \to \phi\ell^+\nu)$ AND $\mathcal{B}(D_s^+ \to \eta'\ell^+\nu)/\mathcal{B}(D_s^+ \to \phi\ell^+\nu)$.

G. Brandenburg,[1] D. Cinabro,[1] T. Liu,[1] M. Saulnier,[1] R. Wilson,[1] H. Yamamoto,[1] T. Bergfeld,[2] B.I. Eisenstein,[2] J. Ernst,[2] G.E. Gladding,[2] G.D. Gollin,[2] M. Palmer,[2] M. Selen,[2] J.J. Thaler,[2] K.W. Edwards,[3] K.W. McLean,[3] M. Ogg,[3] A. Bellerive,[4] D.I. Britton,[4] E.R.F. Hyatt,[4] R. Janicek,[4] D.B. MacFarlane,[4] P.M. Patel,[4] B. Spaan,[4] A.J. Sadoff,[5] R. Ammar,[6] P. Baringer,[6] A. Bean,[6] D. Besson,[6] D. Coppage,[6] N. Copty,[6] R. Davis,[6] N. Hancock,[6] S. Kotov,[6] I. Kravchenko,[6] N. Kwak,[6] Y. Kubota,[7] M. Lattery,[7] M. Momayezi,[7] J.K. Nelson,[7] S. Patton,[7] R. Poling,[7] V. Savinov,[7] S. Schrenk,[7] R. Wang,[7] M.S. Alam,[8] I.J. Kim,[8] Z. Ling,[8] A.H. Mahmood,[8] J.J. O'Neill,[8] H. Severini,[8] C.R. Sun,[8] F. Wappler,[8] G. Crawford,[9] J.E. Duboscq,[9] R. Fulton,[9] D. Fujino,[9] K.K. Gan,[9] K. Honscheid,[9] H. Kagan,[9] R. Kass,[9] J. Lee,[9] M. Sung,[9] C. White,[9] A. Wolf,[9] M.M. Zoeller,[9] X. Fu,[10] B. Nemati,[10] W.R. Ross,[10] P. Skubic,[10] M. Wood,[10] M. Bishai,[11] J. Fast,[11] E. Gerndt,[11] J.W. Hinson,[11] T. Miao,[11] D.H. Miller,[11] M. Modesitt,[11] E.I. Shibata,[11] I.P.J. Shipsey,[11] P.N. Wang,[11] L. Gibbons,[12] S.D. Johnson,[12] Y. Kwon,[12] S. Roberts,[12] E.H. Thorndike,[12] T.E. Coan,[13] J. Dominick,[13] V. Fadeyev,[13] I. Korolkov,[13] M. Lambrecht,[13] S. Sanghera,[13] V. Shelkov,[13] T. Skwarnicki,[13] R. Stroynowski,[13] I. Volobouev,[13] G. Wei,[13] M. Artuso,[14] M. Gao,[14] M. Goldberg,[14] D. He,[14] N. Horwitz,[14] S. Kopp,[14] G.C. Moneti,[14] R. Mountain,[14] F. Muheim,[14] Y. Mukhin,[14] S. Playfer,[14] S. Stone,[14] X. Xing,[14] J. Bartelt,[15] S.E. Csorna,[15] V. Jain,[15] S. Marka,[15] D. Gibaut,[16] K. Kinoshita,[16] P. Pomianowski,[16] B. Barish,[17] M. Chadha,[17] S. Chan,[17] D.F. Cowen,[17] G. Eigen,[17] J.S. Miller,[17] C. O'Grady,[17] J. Urheim,[17] A.J. Weinstein,[17] F. Würthwein,[17] D.M. Asner,[18] M. Athanas,[18] D.W. Bliss,[18] W.S. Brower,[18] G. Masek,[18] H.P. Paar,[18] J. Gronberg,[19] C.M. Korte,[19] R. Kutschke,[19] S. Menary,[19] R.J. Morrison,[19] S. Nakanishi,[19] H.N. Nelson,[19] T.K. Nelson,[19] C. Qiao,[19] J.D. Richman,[19] D. Roberts,[19] A. Ryd,[19] H. Tajima,[19] M.S. Witherell,[19] R. Balest,[20] K. Cho,[20] W.T. Ford,[20] M. Lohner,[20] H. Park,[20] P. Rankin,[20] J.G. Smith,[20] J.P. Alexander,[21] C. Bebek,[21] B.E. Berger,[21] K. Berkelman,[21] K. Bloom,[21] T.E. Browder,[21*] D.G. Cassel,[21] H.A. Cho,[21] D.M. Coffman,[21] D.S. Crowcroft,[21] M. Dickson,[21] P.S. Drell,[21] D.J. Dumas,[21] R. Ehrlich,[21] R. Elia,[21] P. Gaidarev,[21] M. Garcia-Sciveres,[21] B. Gittelman,[21] S.W. Gray,[21] D.L. Hartill,[21] B.K. Heltsley,[21] S. Henderson,[21] C.D. Jones,[21] S.L. Jones,[21] J. Kandaswamy,[21] N. Katayama,[21] P.C. Kim,[21] D.L. Kreinick,[21] T. Lee,[21] Y. Liu,[21] G.S. Ludwig,[21] J. Masui,[21] J. Mevissen,[21] N.B. Mistry,[21] C.R. Ng,[21] E. Nordberg,[21] J.R. Patterson,[21] D. Peterson,[21] D. Riley,[21] A. Soffer,[21] P. Avery,[22] A. Freyberger,[22] K. Lingel,[22] C. Prescott,[22] J. Rodriguez,[22] S. Yang,[22] and J. Yelton[22]

(CLEO Collaboration)
[1] *Harvard University, Cambridge, Massachusetts 02138*
[2] *University of Illinois, Champaign-Urbana, Illinois, 61801*
[3] *Carleton University, Ottawa, Ontario K1S 5B6 and the Institute of Particle Physics, Canada*
[4] *McGill University, Montréal, Québec H3A 2T8 and the Institute of Particle Physics, Canada*
[5] *Ithaca College, Ithaca, New York 14850*
[6] *University of Kansas, Lawrence, Kansas 66045*
[7] *University of Minnesota, Minneapolis, Minnesota 55455*
[8] *State University of New York at Albany, Albany, New York 12222*
[9] *Ohio State University, Columbus, Ohio, 43210*
[10] *University of Oklahoma, Norman, Oklahoma 73019*
[11] *Purdue University, West Lafayette, Indiana 47907*
[12] *University of Rochester, Rochester, New York 14627*
[13] *Southern Methodist University, Dallas, Texas 75275*
[14] *Syracuse University, Syracuse, New York 13244*
[15] *Vanderbilt University, Nashville, Tennessee 37235*
[16] *Virginia Polytechnic Institute and State University, Blacksburg, Virginia, 24061*
[17] *California Institute of Technology, Pasadena, California 91125*
[18] *University of California, San Diego, La Jolla, California 92093*
[19] *University of California, Santa Barbara, California 93106*
[20] *University of Colorado, Boulder, Colorado 80309-0390*
[21] *Cornell University, Ithaca, New York 14853*
[22] *University of Florida, Gainesville, Florida 32611*

Abstract

Using the CLEO II detector at the Cornell Electron Storage Ring (CESR), we observe clean signals in both $D_s^+ \to \eta\ell^+\nu$ and $D_s^+ \to \eta'\ell^+\nu$ decay channels. We measure $\mathcal{B}(D_s^+ \to \eta e^+\nu)/\mathcal{B}(D_s^+ \to \phi e^+\nu) = 1.24 \pm 0.12 \pm 0.15$, $\mathcal{B}(D_s^+ \to \eta' e^+\nu)/\mathcal{B}(D_s^+ \to \phi e^+\nu) = 0.43 \pm 0.11 \pm 0.07$ and $\mathcal{B}(D_s^+ \to \eta' e^+\nu)/\mathcal{B}(D_s^+ \to \eta e^+\nu) = 0.35 \pm 0.09 \pm 0.07$. We find the vector to pseudoscalar ratio, $\mathcal{B}(D_s^+ \to \phi e^+\nu)/\mathcal{B}(D_s^+ \to (\eta+\eta')e^+\nu) = 0.60 \pm 0.06 \pm 0.06$, which is similar to the ratio found in non strange D decays.

PACS numbers: 13.20.Fc, 13.65+i, 14.40.Lb

Typeset using REVTEX

*Permanent address: University of Hawaii at Manoa

One of the outstanding problems in charm semileptonic decay is the disagreement on the vector to pseudoscalar ratio, $\mathcal{B}(D \to \overline{K}^* e^+\nu)/\mathcal{B}(D \to \overline{K} e^+\nu)$. The experimental world average of this ratio is 0.56 ± 0.06 [1], while theoretical predictions range from 0.5 to 1.2 [1,2]. It is of interest to repeat these measurements in the D_s^+ sector, where the initial and final hadrons differ by the substitution of a light quark by a strange quark. In the D_s^+ sector only the $D_s^+ \to \phi\ell^+\nu$ decay has been extensively studied. The Fermilab experiment E653 has seen evidence for the remaining major D_s^+ semileptonic modes, $D_s^+ \to (\eta + \eta')\mu^+\nu$ [3]. In this paper we report the first measurements of $\mathcal{B}(D_s^+ \to \eta e^+\nu)$ and $\mathcal{B}(D_s^+ \to \eta' e^+\nu)$ normalized to $\mathcal{B}(D_s^+ \to \phi e^+\nu)$, and the vector to pseudoscalar ratio. The data include events with both muons and electrons. Phase space corrections have been applied to the muon data to present radiatively corrected electron branching ratios.

The data consists of an integrated luminosity of 3.11 fb^{-1} of e^+e^- collisions recorded with the CLEO II detector at the Cornell Electron Storage Ring (CESR). The data sample contains about 3.7 million $e^+e^- \to c\bar{c}$ events taken at center-of-mass energies on the $\Upsilon(4S)$ resonance and in the nearby continuum ($\sqrt{s} \sim 10.6$ GeV). The CLEO II detector includes a CsI electromagnetic calorimeter that provides excellent η reconstruction [4].

Due to the undetected neutrino, we cannot fully reconstruct $D_s^+ \to X\ell^+\nu$ decays, where $X \equiv \phi$, η or η'. However, there are few processes which produce both an X and a lepton in the same jet. This correlation is used to extract a clean $D_s^+ \to X\ell^+\nu$ signal and is implemented by requiring that the X and the lepton be in the same hemisphere with respect to the thrust axis of the event. Backgrounds can be reduced for $D_s^+ \to \eta\ell^+\nu$ and $D_s^+ \to \phi\ell^+\nu$, which have sufficient statistics, by also detecting the low energy photon from the $D_s^{*+} \to D_s^+\gamma$ decay. We refer to this second method as the D_s^{*+} tag analysis. The two values of $\mathcal{B}(D_s^+ \to \eta e^+\nu)/\mathcal{B}(D_s^+ \to \phi e^+\nu)$ are combined.

Electron and muon candidates are restricted to lie in the fiducial regions $|\cos\theta| < 0.91$ and $|\cos\theta| < 0.81$, respectively, where θ is the polar angle of the track with respect to the beam axis. Electron candidates are required to have momenta above 0.7 GeV/c and 1.0 GeV/c for the D_s^{*+} tag and non D_s^{*+} tag analyses, respectively. Electrons are identified by comparing their ionization energy loss, time-of-flight, energy deposit and shower shapes in the electromagnetic calorimeter with that expected for true electrons. Electrons from photon conversions and Dalitz decays of π^0's are rejected. Muon candidates in the region $|\cos\theta| < 0.61$ are required to have momenta above 1.5 GeV/c, and those in the region $|\cos\theta| > 0.61$ are required to have momenta above 1.9 GeV/c. In order to be identified as a muon, a track must penetrate at least 5 interaction lengths of iron.

We identify ϕ, η and η' candidates by detecting the decays to the K^+K^-, $\gamma\gamma$ and $\eta\pi^+\pi^-$ states, respectively. We require that the momenta of these states be greater than 1.0 GeV/c to reduce combinatoric background. Charged kaon candidates are required to have ionization energy loss and time-of-flight consistent with that expected for true kaons. Momentum dependent efficiencies for identifying kaons in ϕ decays are obtained from the data by comparing the inclusive ϕ yield before and after particle identification. These efficiencies are then combined with the predicted ϕ momentum spectrum from $D_s^+ \to \phi\ell^+\nu$ Monte Carlo events to give the total ϕ identification efficiency. Photon candidates must lie in the fiducial region $|\cos\theta| < 0.81$ and have a lateral shower shape consistent with that expected for true photons. In reconstructing the η we require $|\cos\theta_d| < 0.9$ to reduce random combinations of low momentum photons, where θ_d is the photon decay angle in the η rest frame with respect

to the η direction in the laboratory. We veto any photon which, when combined with another photon, has an invariant mass consistent with the π^0 mass and a momentum greater than 0.8 GeV/c. In reconstructing the η' we require that the invariant mass of the two photons from $\eta \to \gamma\gamma$ decays be consistent with the η mass and the η momentum be greater than 0.5 GeV/c. Charged pion candidates must have ionization energy loss and time-of-flight consistent with that expected for true pions. The pion identification efficiency in η' decays is obtained from the inclusive η' data in the same manner as the kaon identification efficiency for the ϕ reconstruction.

To suppress the combinatoric background from $\Upsilon(4S)$ events, which tend to be more spherical, we require that the ratio of Fox-Wolfram moments [5], $R_2 = H_2/H_0$, be greater than 0.30. The $X\ell^+$ candidates must have an invariant mass less than 1.9 GeV/c^2. For $\eta\ell^+$ candidates we require that the $\eta\ell^+$ invariant mass be greater than 1.2 GeV/c^2 since backgrounds are large at low $\eta\ell^+$ mass. In addition, we require that the $X\ell^+$ momentum be less than 4.5 GeV/c, and greater than 2.0 and 2.5 GeV/c for the D_s^{*+} tag and non tag analyses, respectively. Efficiencies are determined with a Monte Carlo simulation using the ISGW model [6]. These Monte Carlo events are passed through a full simulation of the CLEO II detector and the same event reconstruction and analysis chain as the data.

The K^+K^-, $\gamma\gamma$ and $\eta\pi^+\pi^-$ invariant mass spectra for all $X\ell^+$ combinations which pass the above selection criteria are fit to obtain the number of candidates which are given in Table I. Figures 1(a) and (b) show the invariant mass spectra for $\gamma\gamma$ and $\eta\pi^+\pi^-$.

There are two main sources of background in the sample: X's accompanied by fake leptons [7], and random $X\ell^+$ combinations. The background due to fake leptons is estimated by using the real data to measure the momentum dependent probabilities that a hadron will be misidentified as a lepton. These probabilities are typically 0.3% for electrons and 1.2% for muons. To estimate the number of events due to fake leptons we take the events which pass the basic event selection cuts and treat all charged tracks in these events, which do not pass the lepton identification criteria, as leptons. The entries which pass all the cuts are weighted by the appropriate fake probability and summed to give the fake background given in Table I.

Random $X\ell^+$ combinations come from $e^+e^- \to c\bar{c}$ events in which an X produced in the fragmentation process is combined with a lepton from a semileptonic decay of the charmed hadron in the same jet, and from $\Upsilon(4S) \to B\bar{B}$ events in which an X produced in the decay chain of one of the B mesons is combined with a lepton from a semileptonic decay of the other B meson. The background from random $X\ell^+$ combinations is estimated using the Monte Carlo simulation. However, the X production rate from both fragmentation and B meson decays is not well simulated. For this reason the magnitudes of these backgrounds are determined from the data.

To determine the rate at which fragmentation X's are produced in the same jet as a charmed meson we use a sample containing reconstructed $D^0 \to K^-\pi^+$ decays with D^0 momenta in the same range as those of our D_s^+ sample. Since leptons come primarily from charm semileptonic decays, the direction of a charmed hadron is close to that of the high momentum lepton. The yields of D^0 and X mesons produced in the same hemisphere are obtained by fitting their invariant mass distributions. In order to improve statistics we lower the X momentum cut to 0.8 GeV/c. In data 1.2 ± 0.5 η mesons are found for every 1000 reconstructed D^0 mesons. This is to be compared with 1.7 ± 0.1 η mesons per 1000 D^0 mesons

in the $e^+e^- \to c\bar{c}$ Monte Carlo sample. Therefore for $D_s^+ \to \eta\ell^+\nu$ we scale the Monte Carlo estimate of the charm continuum background by the factor of 0.7 ± 0.3. The scale factors for $D_s^+ \to \phi\ell^+\nu$ and $D_s^+ \to \eta'\ell^+\nu$ are 1.0 ± 0.7 and $0.0^{+0.4}_{-0.0}$, respectively. With these factors applied, the Monte Carlo simulation predicts the continuum $c\bar{c}$ background given in Table I.

The background from random $X\ell^+$ combinations in $B\bar{B}$ events is estimated in a similar manner. In this case the directions of the X and the lepton are uncorrelated. Therefore we compare the number of X's with momentum above 1.0 GeV/c in the continuum subtracted $\Upsilon(4S)$ data with the number observed in the $\Upsilon(4S)$ $B\bar{B}$ Monte Carlo sample. The resulting backgrounds are found by scaling the Monte Carlo estimate and the results are given in Table I.

For $D_s^+ \to \eta\ell^+\nu$ decay, we estimate the $D_s^+ \to \eta'\ell^+\nu$ feed down by multiplying the efficiency corrected yield of the $D_s^+ \to \eta'\ell^+\nu$ decay in our data sample, as discussed below, by the appropriate efficiency and the branching fraction. The Cabibbo suppressed $D^+ \to \eta\ell^+\nu$ decay contributes a sizable contamination to the $D_s^+ \to \eta\ell^+\nu$ decay in the non D_s^{*+} tag analysis since we cannot distinguish D^+ from D_s^+ decays. We estimate the ratio of the numbers of $D^+ \to \eta\ell^+\nu$ and $D_s^+ \to \eta\ell^+\nu$ events, $R_c^\eta \equiv N(D^+ \to \eta\ell^+\nu)/N(D_s^+ \to \eta\ell^+\nu) = 0.17 \pm 0.07$ [8]. The final signal yield for $D_s^+ \to \eta\ell^+\nu$ decay is $N_{signal} = (N_{candidates} - N_{fake\ lepton} - N_{c\bar{c}} - N_{B\bar{B}} - N_{D_s^+ \to \eta'\ell^+\nu}) \cdot f_c^\eta$ where $f_c^\eta \equiv 1/(1 + R_c^\eta)$. The signal yield for the $D_s^+ \to \eta'\ell^+\nu$ decay is calculated in the same manner. The results are given in Table I.

Figures 1(c) and (d) show the fitted number of η's and η''s which fall in each bin of the $\eta\ell^+$ and $\eta'\ell^+$ mass, respectively. The combined background estimate is also shown, as well as the sum of the simulated signal and the combined background estimate. The simulated signal has been normalized to the number of candidates extracted from the fit to the $\gamma\gamma$ and $\eta\pi^+\pi^-$ invariant mass spectra. Table I gives the yields after correcting for efficiencies and the $\phi \to K^+K^-$, $\eta \to \gamma\gamma$ and $\eta' \to \eta\pi^+\pi^-$ branching fractions.

In the D_s^{*+} tag analysis, we look for a low energy photon from the $D_s^{*+} \to D_s^+\gamma$ decay in the same jet as the $X(\equiv \phi$ or $\eta)$ and the lepton. The photon candidate must lie in the fiducial region $|\cos\theta| < 0.71$, and have energy greater than 0.12 GeV. We require that the lateral shower shape of the photon candidate be consistent with that expected for a true photon. To further suppress background photons from π^0 decays, we veto any photon that has an invariant mass consistent with the π^0 mass when combined with another photon. To select $X\ell^+\gamma$ candidates we require that $\Delta M \equiv M_{X\ell^+\gamma} - M_{X\ell^+}$ be between 0.1 and 0.2 GeV/c^2, where $M_{X\ell^+}$ and $M_{X\ell^+\gamma}$ are the invariant masses of $X\ell^+$ and $X\ell^+\gamma$ systems, respectively. Figure 2(a) and (b) show the K^+K^- and $\gamma\gamma$ invariant mass spectra for all $\phi\ell^+\gamma$ and $\eta\ell^+\gamma$ combinations which pass the above selection criteria. The number of candidates found in these modes are given in Table I.

The backgrounds due to fake leptons, random $X\ell^+$ combinations, and the $D_s^+ \to \eta'\ell^+\nu$ feed down are estimated by the same procedures as for the non D_s^{*+} tag analysis. The contamination from the Cabibbo suppressed decay $D^+ \to \eta\ell^+\nu$ is estimated to be small compared with that for the non D_s^{*+} tag analysis. These backgrounds are listed in Table I. The background from the combination of a true $X\ell^+$ and a random photon is estimated using a Monte Carlo simulation. To test the agreement between the Monte Carlo estimate and the data for this background, we use events with the decay chain, $D^{*+} \to D^0\pi^+$ and $D^0 \to K^-e^+\nu$. These events are ideally suited for the test because a K^-e^+ pair has kinematics similar to that of an $X\ell^+$ pair from the D_s^+ decay. We combine photons with K^-e^+ pairs

TABLE I. Summary of the non D_s^{*+} and D_s^{*+} tag analyses. The errors quoted in this table are statistical only. To get the corrected yield, we divide the signal yield by the detection efficiency (ϵ) and the branching fraction ($\mathcal{B}$) for the subsequent decays of ϕ, η or η' mesons, and a factor of two to take into account the fact that the lepton can be either electron or muon.

	non D_s^{*+} tag			D_s^{*+} tag	
Decay mode	$D_s^+ \to \phi\ell^+\nu$	$D_s^+ \to \eta\ell^+\nu$	$D_s^+ \to \eta'\ell^+\nu$	$D_s^+ \to \phi\ell^+\nu$	$D_s^+ \to \eta\ell^+\nu$
Candidates	863.6 ± 40.5	577.6 ± 30.3	42.3 ± 7.9	326.9 ± 27.1	153.4 ± 15.0
Fake lepton	95.3 ± 2.2	128.8 ± 1.6	9.0 ± 0.4	27.9 ± 1.2	22.7 ± 0.7
$c\bar{c}$	23.1 ± 0.8	35.1 ± 2.0	0.0 ± 0.0	15.6 ± 0.7	8.5 ± 1.0
$B\bar{B}$	49.6 ± 1.8	27.6 ± 2.5	1.9 ± 0.2	7.9 ± 0.7	3.8 ± 1.0
$D_s^+ \to \eta'\ell^+\nu$		5.0 ± 1.3			2.3 ± 0.6
$D_s^+ + D^+$	695.6 ± 40.6	381.0 ± 30.5	31.4 ± 7.9		
f_c		0.855	0.926		
D_s^+ signal yield	695.6 ± 40.6	325.6 ± 26.1	29.1 ± 7.3		
$D^+ \to \eta\ell^+\nu$					1.3 ± 0.1
D_s^{*+} + Random photon				275.5 ± 27.2	114.8 ± 15.1
f_{sig}				0.759	0.803
D_s^{*+} signal yield				209.2 ± 20.6	92.2 ± 12.1
$\epsilon \cdot \mathcal{B}(\%)$	2.078	0.807	0.204	1.408	0.474
Corrected yield	16734 ± 976	20184 ± 1616	7128 ± 1786	7431 ± 733	9730 ± 1276

selected with the same criteria as for $X\ell^+$'s from the D_s^+ decay. In data 21.4 ± 1.7 $K^-e^+\gamma$'s are found for every 100 reconstructed K^-e^+ pairs. This is to be compared with 22.3 ± 0.1 $K^-e^+\gamma$'s per 100 K^-e^+ pairs in the Monte Carlo sample. Therefore we scale the Monte Carlo estimate of the random photon background by the factor of 0.96 ± 0.08. With this scale factor, the Monte Carlo simulation predicts the ratio of the signal to the sum of the signal and the random photon background, f_{sig}, to be 0.759 ± 0.030 for $D_s^+ \to \phi\ell^+\nu$ and 0.803 ± 0.031 for $D_s^+ \to \eta\ell^+\nu$. The results are given in in Table I. Figures 2(c) and (d) show the fitted number of ϕ's and η's which fall in each ΔM bin, respectively. The combined background estimate is also shown, as well as the sum of the simulated signal and the combined background estimate. The simulated signal has been normalized to the number of candidates extracted from the fit to the K^+K^- and $\gamma\gamma$ invariant mass spectra.

To obtain the effective branching ratio in the electron channel, we take into account the reduced phase space for the muon channel [9], and the efficiency loss due to the final state radiation for the electron channel [10]. The results of these analyses presented as ratios of branching ratios are given in Table II for η/ϕ and in Table III for η'/ϕ and η'/η. The non tag measurement is statistically more significant than the tag measurement, but it has a larger systematic uncertainty due to the $D^+ \to \eta\ell^+\nu$ contamination. The two measurements for η/ϕ are combined taking into account the correlated statistical and systematic errors to attain the result given in Tables II and III. The major contributions to the systematic error in $\mathcal{B}(D_s^+ \to \eta e^+\nu)/\mathcal{B}(D_s^+ \to \phi e^+\nu)$ are the uncertainties in the $D^+ \to \eta\ell^+\nu$ contam-

ination, fitting, fake lepton, and charm continuum backgrounds. The systematic errors in $\mathcal{B}(D_s^+ \to \eta' e^+\nu)/\mathcal{B}(D_s^+ \to \phi e^+\nu)$ and $\mathcal{B}(D_s^+ \to \eta' e^+\nu)/\mathcal{B}(D_s^+ \to \eta e^+\nu)$ are dominated by the uncertainty in the charm continuum background.

TABLE II. Summary of $\mathcal{B}(D_s^+ \to \eta e^+\nu)/\mathcal{B}(D_s^+ \to \phi e^+\nu)$ measurements

	$\frac{\mathcal{B}(D_s^+ \to \eta e^+\nu)}{\mathcal{B}(D_s^+ \to \phi e^+\nu)}$
non D_s^{*+} tag	$1.21 \pm 0.12 \pm 0.16$
D_s^{*+} tag	$1.32 \pm 0.22 \pm 0.15$
combined	$1.24 \pm 0.12 \pm 0.15$

Model predictions and measurements are listed in Table III. Our measurements of $\mathcal{B}(D_s^+ \to \eta e^+\nu)/\mathcal{B}(D_s^+ \to \phi e^+\nu)$ and $\mathcal{B}(D_s^+ \to \eta' e^+\nu)/\mathcal{B}(D_s^+ \to \phi e^+\nu)$ agree well with the ISGW2 model predictions with an $\eta - \eta'$ mixing angle of $-10°$ [11]. Our measurement of the vector to pseudoscalar ratio for the D_s^+ semileptonic decays, $0.60 \pm 0.06 \pm 0.06$, agrees well with the measurements for D semileptonic decays, 0.56 ± 0.06 [1], and also with the ISGW2 model prediction [11]. Using the factorization hypothesis, Kamal *et al.* predict $\mathcal{B}(D_s^+ \to \eta' e^+\nu)/\mathcal{B}(D_s^+ \to \eta e^+\nu) = \mathcal{B}(D_s^+ \to \eta' \rho^+)/\mathcal{B}(D_s^+ \to \eta \rho^+)$ [12]. We obtain $\mathcal{B}(D_s^+ \to \eta' \rho^+)/\mathcal{B}(D_s^+ \to \eta \rho^+) = 1.20 \pm 0.35$ from the CLEO measurements [13]. This disagrees with our measurement of $\mathcal{B}(D_s^+ \to \eta' e^+\nu)/\mathcal{B}(D_s^+ \to \eta e^+\nu) = 0.35 \pm 0.09 \pm 0.07$.

TABLE III. Summary of measurements and predictions. The numbers in (parentheses) [brackets] are the ISGW2 predictions using values of the $\eta - \eta'$ mixing angle of $(-10°)$ and $[-20°]$.

	This Experiment	E653	ISGW2
$\frac{\mathcal{B}(D_s^+ \to \eta e^+\nu)}{\mathcal{B}(D_s^+ \to \phi e^+\nu)}$	$1.24 \pm 0.12 \pm 0.15$		(1.17)[0.77]
$\frac{\mathcal{B}(D_s^+ \to \eta' e^+\nu)}{\mathcal{B}(D_s^+ \to \phi e^+\nu)}$	$0.43 \pm 0.11 \pm 0.07$	< 1.6 @90%C.L.	(0.50)[0.67]
$\frac{\mathcal{B}(D_s^+ \to \eta' e^+\nu)}{\mathcal{B}(D_s^+ \to \eta e^+\nu)}$	$0.35 \pm 0.09 \pm 0.07$		(0.43)[0.86]
$\frac{\mathcal{B}(D_s^+ \to \phi e^+\nu)}{\mathcal{B}(D_s^+ \to (\eta+\eta') e^+\nu)}$	$0.60 \pm 0.06 \pm 0.06$	$0.26^{+0.18}_{-0.07}$	(0.60)[0.69]

In conclusion, we have measured $\mathcal{B}(D_s^+ \to \eta e^+\nu)/\mathcal{B}(D_s^+ \to \phi e^+\nu) = 1.24 \pm 0.12 \pm 0.15$ and $\mathcal{B}(D_s^+ \to \eta' e^+\nu)/\mathcal{B}(D_s^+ \to \phi e^+\nu) = 0.43 \pm 0.11 \pm 0.07$. Our value for the ratio of vector to pseudoscalar rates for the D_s^+ semileptonic decays agrees with that observed for the D semileptonic decays, and also with the ISGW2 model prediction. This agreement increases confidence in the evaluations of the $D_s^+ \to \phi\pi^+$ branching ratio using models of semileptonic decays and measurements of $\Gamma(D_s^+ \to \phi\ell^+\nu)/\Gamma(D_s^+ \to \phi\pi^+)$ [1,2].

We gratefully acknowledge the effort of the CESR staff in providing us with excellent luminosity and running conditions. This work was supported by the National Science Foundation, the U.S. Department of Energy, the Heisenberg Foundation, the Alexander von

Humboldt Stiftung, the Natural Sciences and Engineering Research Council of Canada, and the A.P. Sloan Foundation.

REFERENCES

[1] Particle Data Group, L. Montanet *et al.*, Review of Particle Properties, Phys. Rev. D **50**, 1565 (1994).

[2] J.D. Richman and P.R. Burchat, preprint UCSB-HEP-95-08 & Stanford-HEP-95-01, to be published in Reviews of Modern Physics.

[3] E653 Collaboration, K. Kodama *et al.*, Phys. Lett. B **309**, 483 (1993).

[4] CLEO Collaboration, Y. Kubota *et al.*, Nucl. Instrum. Methods Phys. Res., Sect. A **320**, 66 (1992).

[5] G.C. Fox and S. Wolfram, Phys. Rev. Lett. **41**, 1581 (1978).

[6] N. Isgur *et al.*, Phys. Rev. D **39**, 799 (1989).

[7] Fake leptons are either misidentified hadrons or muons from π^+ and K^+ decays in flight.

[8] The ratio of the numbers of $D^+ \to \eta(\eta')\ell^+\nu$ and $D_s^+ \to \eta(\eta')\ell^+\nu$ events can be written as: $R_c^{\eta}(R_c^{\eta'}) = \frac{\sigma(D^+)}{\sigma(D_s^+)} \cdot \frac{\Gamma(D^+ \to \eta(\eta')\ell^+\nu)}{\Gamma(D_s^+ \to \eta(\eta')\ell^+\nu)} \cdot \frac{\tau_{D^+}}{\tau_{D_s^+}}$. Combining the measurement for $\frac{\sigma(D^+)\cdot\mathcal{B}(D^+ \to K^-\pi^+\pi^+)}{\sigma(D_s^+)\cdot\mathcal{B}(D_s^+ \to \phi\pi^+)}$ [14], the CLEO measurement for $\mathcal{B}(D^+ \to K^-\pi^+\pi^+)$ [15] and the world average for $\mathcal{B}(D_s^+ \to \phi\pi^+)$ [16], we obtain $\sigma(D^+)/\sigma(D_s^+) = 2.5 \pm 0.6$. ISGW2 predicts $\Gamma(D^+ \to \eta(\eta')\ell^+\nu)/\Gamma(D_s^+ \to \eta(\eta')\ell^+\nu)$ for values of the $\eta - \eta'$ mixing angle of $-10°$ and $-20°$ [11]. Using the world averages for the D^+ and D_s^+ lifetimes [16], we estimate $R_c^{\eta}(R_c^{\eta'}) = 0.17 \pm 0.07$ (0.08 ± 0.03) for an $\eta - \eta'$ mixing angle of $-15° \pm 5°$.

[9] J.G. Körner and G.A. Schuler, Z. Phys. C **46**, 93 (1990).

[10] D. Atwood and W.J. Marciano, Phys. Rev. D **41**, 1736 (1990).

[11] D. Scora and N. Isgur, preprint CEBAF-TH-94-14.

[12] A.N. Kamal *et al.*, Phys. Rev. D **49**, 1330 (1994).

[13] CLEO Collaboration, P. Avery *et al.* Phys. Rev. Lett. **68**, 1279 (1992).

[14] CLEO Collaboration, P. Avery *et al.*, preprint CLNS 90-992.

[15] CLEO Collaboration, R. Balest *et al.*, Phys. Rev. Lett. **72**, 2328 (1994).

[16] Particle Data Group, L. Montanet *et al.*, Review of Particle Properties, Phys. Rev. D **50**, 1173 (1994).

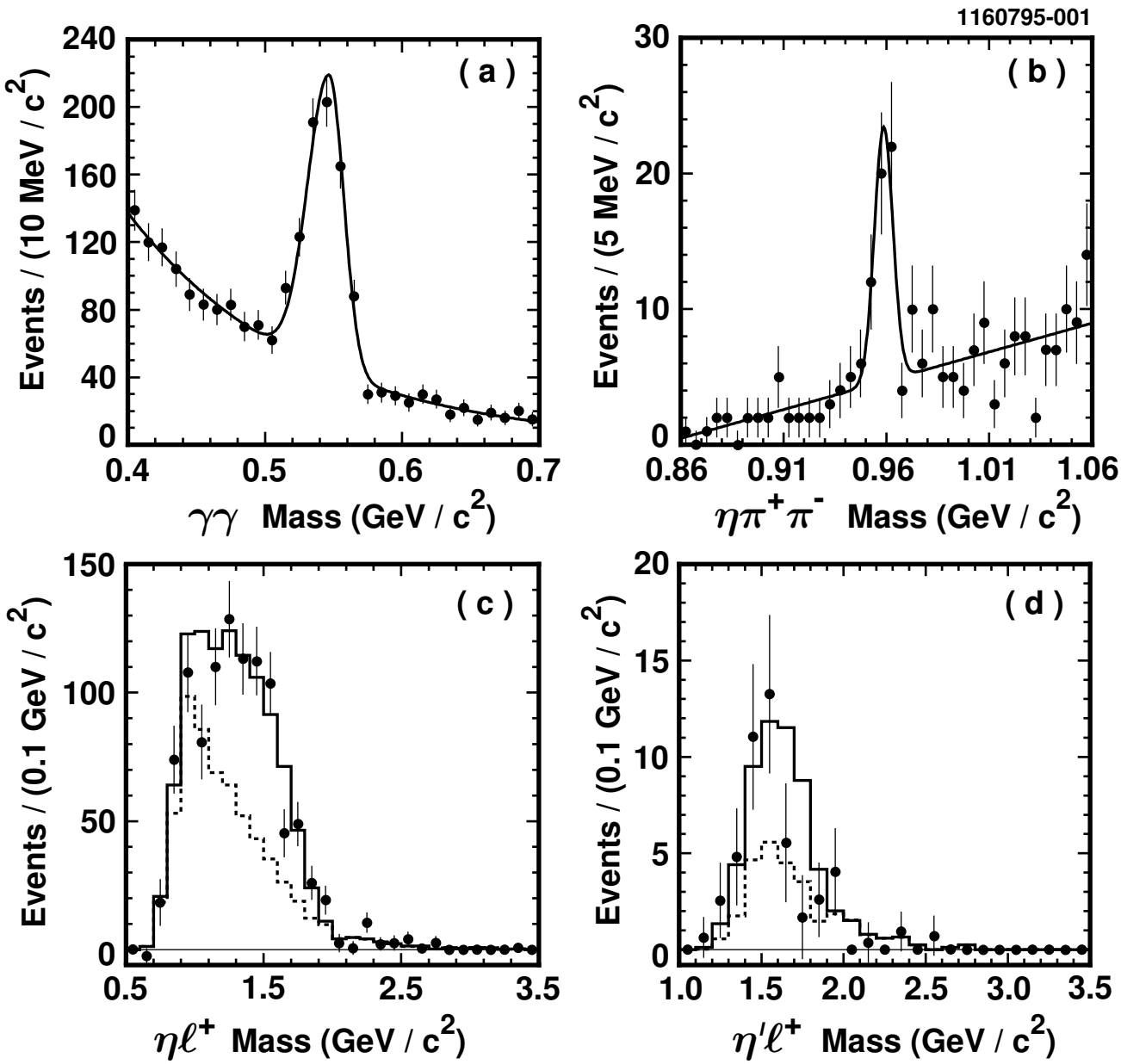

FIG. 1. The (a) $\gamma\gamma$ and (b) $\eta\pi^+\pi^-$ invariant mass spectra for $D_s^+ \to \eta\ell^+\nu$ and $D_s^+ \to \eta'\ell^+\nu$ candidates in the non D_s^{*+} tag analysis: The solid curve is a fit to each spectrum. The (c) $\eta\ell^+$ and (d) $\eta'\ell^+$ invariant mass spectra for the candidates: The points with error bars represent the number of candidates in each mass bin. The solid histogram shows the simulated signal plus the predicted background, and the dotted histogram shows the predicted background. We removed the cut on $\eta\ell^+$ and $\eta'\ell^+$ invariant masses discussed in the text for (c) and (d).

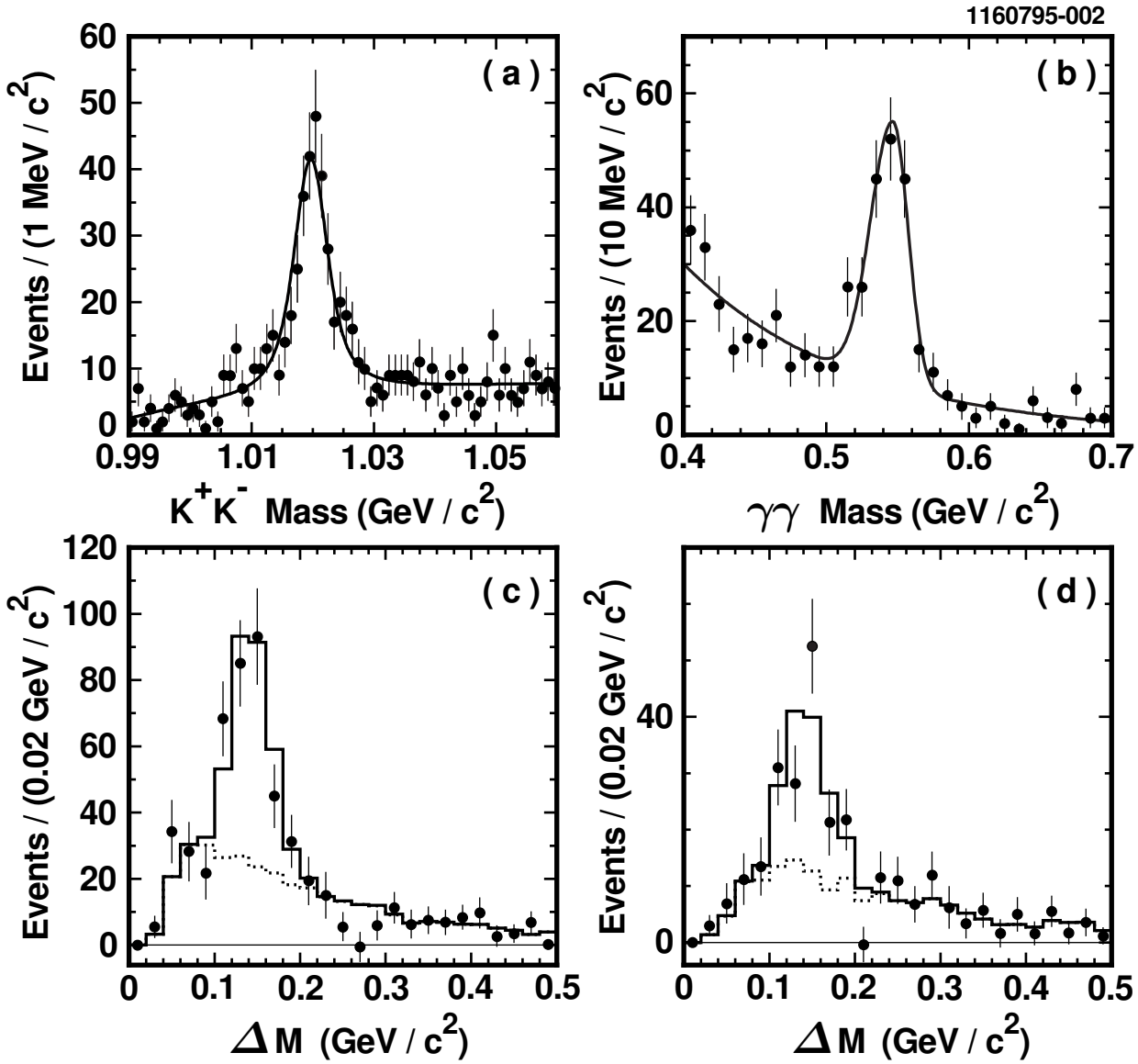

FIG. 2. The (a) K^+K^- and (b) $\gamma\gamma$ invariant mass spectra for $D_s^+ \to \phi\ell^+\nu$ and $D_s^+ \to \eta\ell^+\nu$ candidates in the D_s^{*+} tag analysis: Note that a candidate photon from the D_s^{*+} is required. The solid curve is a fit to each spectrum. The spectra of the pseudo mass difference ΔM for (c) $D_s^+ \to \phi\ell^+\nu$ and (d) $D_s^+ \to \eta\ell^+\nu$ candidates: The points with error bars represent the number of candidates in each ΔM bin. The solid histogram shows the simulated signal plus the predicted background, and the dotted histogram shows the predicted background. We removed the cut on ΔM discussed in the text for (c) and (d).